

Effect of graphene on properties of acrylic emulsion intumescent fire retardant coating

Mac Van Phuc^{*}, Dao Phi Hung, Nguyen Anh Hiep, Nguyen Thien Vuong, Trinh Van Thanh

*Institute for Tropical Technology, Vietnam Academy of Science and Technology,
18 Hoang Quoc Viet, Cau Giay, Ha Noi, Viet Nam*

^{*}Email: phucmv@itt.vast.vn

Received: 25 January 2022; Accepted for publication: 18 June 2022

Abstract. Nowadays, intumescent paint is one of the most popular fireproof paint products and is widely used in buildings. They can be applied to steel, wood, concrete, etc. This study aimed to enhance the properties of intumescent coating by graphene addition. The effect of graphene (GR) content on fire resistance, thermal and mechanical properties of water-based intumescent coatings were studied. Intumescent coating formulations include acrylic emulsion binder (R4152), flame retardant additives (Ammonium polyphosphate (APP) - acid source, pentaerythritol (PER) - carbon source, melamine (MEL) - foaming source), fire retardant fillers (TiO_2 , $\text{Al}(\text{OH})_3$) were prepared by mixing different graphene content (0.5, 1, 1.5 and 2 wt.% GR). The investigated coating properties were examined by fire protection test, furnace test, static water immersion test, scanning electron microscopy (SEM), thermogravimetric analysis (TGA), differential scanning calorimetry (DSC) and mechanical properties (adhesion, pendulum hardness). The results showed that the GR could effectively enhance the fire resistance performance (from 13.6 % to 23.4 %), thermal stability (from 2.9 % to 5.2 %), water resistance (from 5.0 % to 11.9 %), and mechanical properties (from 5 % to 12 %) of the coating.

Keywords: Intumescent coating, acrylic emulsion, graphene, fire resistance.

Classification numbers: 2.5.3

1. INTRODUCTION

Intumescent paint is one of the current fireproof paint products used widely in industrial and residential buildings, especially for load-bearing structures such as steel and concrete [1]. When heated to high temperatures, intumescent coatings swell to generate a char foam layer that insulates the flame and substrate and limits fire propagation [2]. The advantages of intumescent coatings include the ability to be applied on various materials responding to fire protection, decorative and protective demands. With such unique features, intumescent coatings help protect the structure of the building from being broken, increasing the escape time for victims and minimizing repair costs after the fire [2, 3].

A basic intumescent coating formula consists of the main components: a polymer binder and a system of flame retardant additives, including an acid source (such as ammonium polyphosphate - APP), a blowing agent or foaming agent (such as melamine - MEL) and a carbon source (such as pentaerythritol - PER) [4]. The carbonization mechanism of intumescent coating is described as follows: when the coating is heated to about 250 °C, APP decomposes to

produce phosphoric acid, which reacts with PER to form a carbon char on the surface through dehydration. As carbon char is forming, the MEL begins to decompose and release non-flammable gases such as N_2 , NH_3 . These gases are trapped in the viscous liquid and form bubbles, which cause the carbon char to foam, thus forming a multi-compartment protective char. The new char foam acts as a barrier insulating the protected element from the flame [5, 6].

However, the char layer formed by the APP-PER-MEL system has weak oxidation resistance at high temperatures, leading to low flame retardant efficiency and easy destruction during combustion [7]. Therefore, some flame retardant fillers or additives have been used to enhance the heat shielding effect and make the carbon char more compact of intumescent coatings, such as calcium carbonate, aluminium hydroxide and silica [8, 9]. Carbon materials family (Figure 1) are one of the interesting research directions for fireproof additives due to their excellent chemical and mechanical properties. Graphene (GR) is considered the basic element. It can be stacked to form three-dimensional graphite by interlayer force or rolled to form single-walled or multi-walled carbon nanotubes by an external force. It can also be wrapped into a zero-dimensional fullerene. All these carbon materials have good carbonization and outstanding shielding. These capabilities make the coating more fire- and corrosion-resistant [10, 11].

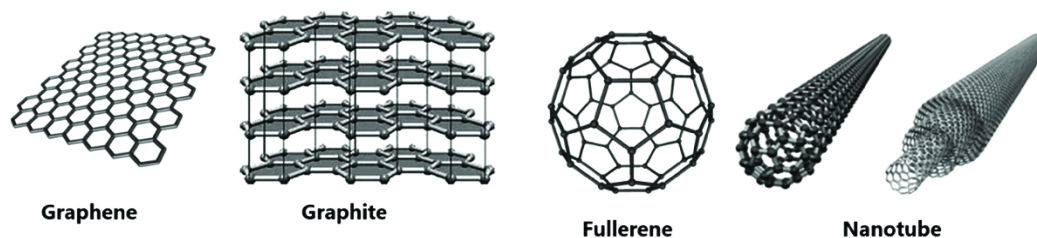


Figure. 1. Structure of various carbon materials.

Graphene has a 2D hexagonal lattice structure composed of carbons with sp^2 hybridization with partitioned p electrons exhibiting unique properties compared to other carbon materials [12]. Graphene exhibits high specific surface area ($\approx 2600 \text{ m}^2/\text{g}$), thermal ($2000 \div 5000 \text{ W/mK}$), electrical conductivity ($\approx 10^{-8} \text{ }\Omega/\text{m}$), and mechanical strength ($\approx 1050 \text{ GPa}$ of Young modulus, 130 GPa of tensile strength) [13, 14]. Graphene has been used as a flame retardant nanoscale additive for thermoplastic and thermosetting polymers [15]. Several studies indicated that GR improved the coating's thermal stability, smoke suppression, and char content [10, 16].

In intumescent coatings, the binder is a crucial component, helping to make the coating uniform and contributing to the formation and expansion of the char layer [4]. Solvent-based coatings have the advantage of better temperature and humidity resistance than water-based coatings. However, concerns about volatile organic compounds (VOCs) have increased the use of water-based coatings as an alternative to solvent-based coatings [9]. Acrylic polymer emulsions are attractive waterborne binders because they can provide UV resistance, water resistance, and good adhesion on many materials such as walls, wood, and metal. Our previous research prepared the coating by mixing acrylic polymer emulsions Plextol R4152 and 0.5 wt.% graphene oxide, enhancing the falling sand abrasion resistance and thermal stability [17].

This study investigated the effect of graphene content on intumescent coating properties. Intumescent coatings contained Plextol R4152 as a binder, APP-PER-MEL as a flame retardant additive system, TiO_2 , $Al(OH)_3$ as fillers, and other additive. The fire resistance test and furnace test were conducted. TGA, DSC, and SEM were used to assess the coating and char layers. The water resistance and mechanical properties of the coatings were examined.

2. MATERIALS AND METHODS

2.1. Materials

Acrylic emulsion Plextol R4152 was provided by Symthomer, having 49 ± 1 % of solid content. APP, PER and MEL were purchased from CF-Chem Co., Ltd. Graphene (industrial grade) was obtained from Applied Nanotechnology JSC, Viet Nam with a diameter of 10-20 μm , thickness < 15 nm, carbon content ≥ 98 %. Aluminium hydroxide and titanium dioxide (rutile), were supplied by Aladdin Industrial Co., Ltd. Triton X-405 (70 %) surfactant were purchased from Sigma Aldrich. Texanol coalescing agent obtained from Dow Chemical Co. Drewplus T 4507A foam control agent was supplied from Ashland Global Holdings Inc. Deionized water was homemade in the laboratory. The SEM photos of GR are shown in Figure 2.

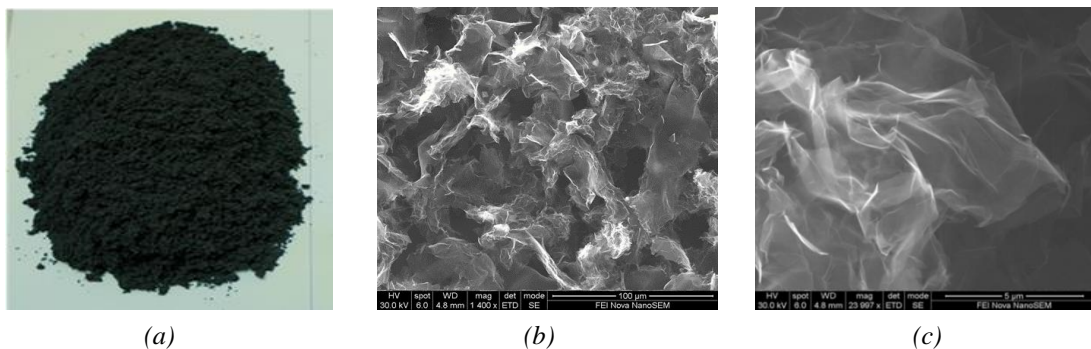


Figure 2. Graphene powder (a), SEM images of graphene at 1.400x (b) and 24.000x magnification (c).

2.2. Sample preparation

The coating compositions are listed in Table 1. The intumescent coating was prepared using the following process: GR was dispersed with surfactant in the deionized water by ultrasonic dispersion (Branson 450 Digital Sonifier) for 2 hours. Next, the high-speed disperser (IKA RW16 Basic) stirred APP, PER, MEL and fillers (TiO_2 , $\text{Al}(\text{OH})_3$) at 800 rpm/min for 1 hour. Finally, acrylic emulsion R4152 and additives (coalescing, foam control) were incorporated into the slurry and stirred for 1 hour at 500 rpm/min. The coatings were coated on SS400 steel plates at 2 ± 0.2 mm thickness. After that, the coatings were dried at room temperature for seven days.

Table 1. The components of the coatings (wt. %).

No	Components	M-0	M-0.5GR	M-1GR	M-1.5GR	M-2GR
1	Acrylic emulsion	38	38	38	38	38
2	APP/PER/MEL	18/9/9	18/9/9	18/9/9	18/9/9	18/9/9
3	$\text{TiO}_2 / \text{Al}(\text{OH})_3$	5/5	5/5	5/5	5/5	5/5
4	Graphene	0	0,5	1	1,5	2
5	Deionized water	15	14.5	14	13.5	13
6	Additives	1	1	1	1	1

2.3. Analysis

2.3.1. Fire resistance test

The fire resistance test was conducted for 2 h by the Bunsen burner is shown in Figure 3.

The coatings were applied to 150 mm × 150 mm × 5 mm SS400 steel plates. The temperature of the sample's backside was recorded by the Testo 925 - type K thermometer during the test.

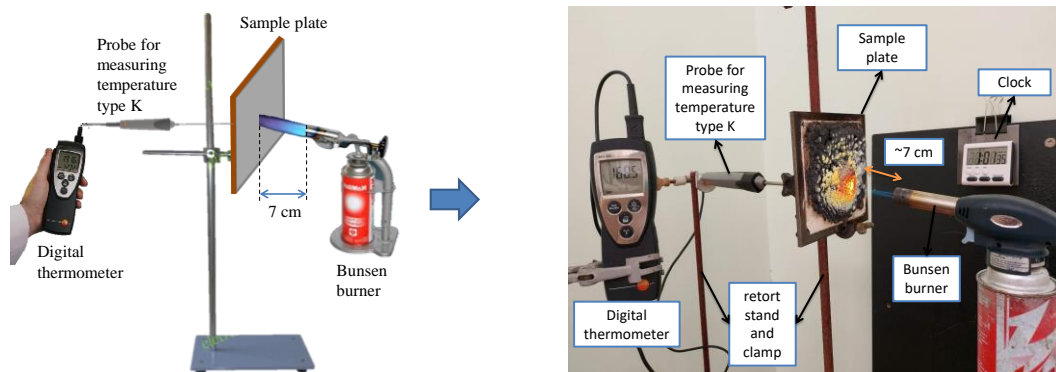


Figure 3. Schematic of the experimental setup for fire resistance test.

2.3.2. Furnace test

The furnace test was conducted to determine the swelling of the coating. The coatings were applied to 100 mm × 100 mm × 5 mm SS400 steel plates. In the furnace test, progressive heating with 10 °C/min rate from room temperature to 800 °C. The temperature was kept at 800 °C for 30 min before cooling to room temperature. The intumescent factor (I) was calculated according to the following Equation 1:

$$I = d_2 / d_1 \quad (1)$$

where d_1 is the thickness of the coating before the furnace test; d_2 is the thickness of the expanded char layer after the furnace test.

2.3.3. Morphology

The morphological structure of coatings and char layer was observed by using scanning electron microscope (SEM) JSM-6510LV (Jeol Company - Japan).

2.3.4. Thermogravimetric analysis

Thermogravimetric analysis was determined by TGA 209F1 (NETZSCH - Germany). The sample was heated from ambient temperature to 800 °C at heating rate of 10 °C/min in the air.

2.3.5. Differential scanning calorimetry

Differential scanning calorimetry was determined using DSC204F1 (NETZSCH - Germany) in the air with a 20 °C/min heating rate from room temperature to 450 °C.

2.3.6. Static immersion test

Static immersion tests measured the water resistance of the coating. Coating samples formed 50 mm x 20 mm x 2 mm bars. The samples were immersed in distilled water at room temperature and removed after specified time intervals. Tissue paper was used to remove extra water from the sample. The water uptake ratio (E_{sw}) for each coating sample was calculated by using Equation 2:

$$E_{sw} (\%) = [(W_a - W_b) / W_b] \times 100 \% \quad (2)$$

where W_b is the weight of the coating sample before water immersion (g); W_a is the dry weight of the coating sample after water immersion (g).

2.3.7. Mechanical properties

- *Adhesion strength*: The adhesion strength of the coatings on the concrete substrate was determined by using the pull-off adhesion tester (PosiTest-AT-A Automatic, DeFelsko). The adhesion strength (X) for samples was calculated using Equation 3:

$$X = 4F/\pi d^2 \quad (3)$$

where X is the pull-off load achieved at fracture (MPa); F is the actual load applied to the test (N); d is the diameter of the loading fixture (mm).

- *Pendulum hardness*: The pendulum hardness was determined by measuring the damping of the Persoz pendulum on the coatings using a Pendulum Damping Tester (model 299/300 - Erichsen). Investigated coatings were fabricated by Film Applicator model 306 (Erichsen) on the glass plate with a wet thickness of 120 μm . The pendulum hardness value is the ratio between the number of oscillations placed on the coated glass and the reference glass.

3. RESULTS AND DISCUSSION

3.1. Fire resistance test

Fire resistance is an essential indicator in evaluating the performance of intumescent fire-protective coatings. The fire resistance of intumescent coatings filled with different graphene content is shown in Figure 4. Photographs of the residual carbon of coatings after the fire resistance test are shown in Figure 5.

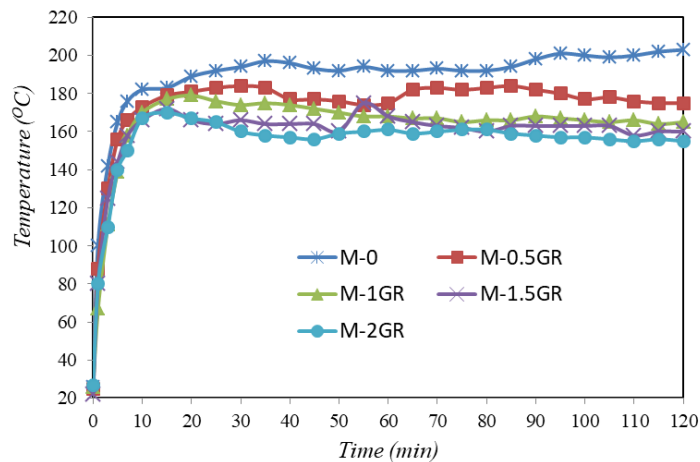


Figure 4. Influence of GR content on fire resistance of coatings.

Figure 4 shows that all coatings increased quickly and exceeded 160 °C in the first 7 minutes, then increased slowly. All the coating samples showed a similar rise in temperature resulting from thermal degradation and the formation of char layers from chemical reactions between the coating ingredients [18]. After 15 minutes of fire exposure, almost all the samples attained equilibrium temperature and remained unchanged, except the M-0 increased until it reached 200 °C after 30 minutes.

After 120 minutes of the fire test, the final temperature of M-0, M-0.5GR, M-1GR, M-1.5GR and M-2GR coating samples were 203.6 °C, 175.8 °C, 165.5 °C, 160.3 °C and 155.9 °C, respectively. The obtained results indicated that adding graphene increased the fire resistance,

decreasing the heat transmitted to the surface of the steel substrate below, and the M-2GR sample gave the best results.

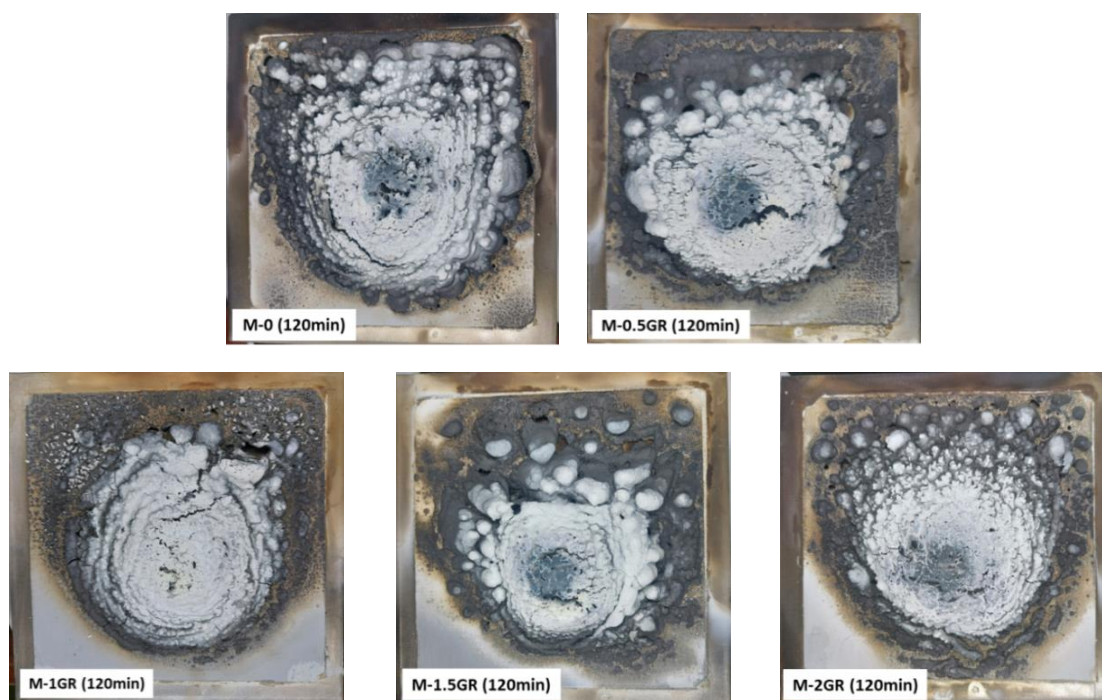


Figure 5. The residual carbon photographs of coatings after fire resistance test.

It can be seen from Figure 5 that after 120 minutes of the fire test, all samples had some cracks and collapses. The collapses are located at the direct flame contact position, possibly due to the Bunsen burner's gas pressure. The coating surface without graphene (M-0) had more numerous and deeper than other samples containing graphene, leading to more fire and heat transfer to the steel substrate. These results showed that graphene has improved the fire resistance of the coatings by inhibiting the two main factors of combustion, i.e., heat and material. In particular, graphene, which has a unique two-dimensional layered structure, is stable at high temperatures due to its ability to absorb large amounts of heat.

Moreover, graphene could act as a mold for char, promoting the formation of stacked char layers and creating a "labyrinth" effect. As a result, graphene prevents heat transfer from the heat source into the material. In addition, graphene with a large specific surface area can adsorb or prevent flammable volatile release and diffusion during combustion [19].

However, the temperature of M-1GR, M-1.5GR and M-2GR samples was not much different. The reason may be that when the graphene content was increased, the phenomenon of graphene agglomeration in the coating occurred, resulting in the coating's dispersion and flame retardant performance were not much better than each other [15].

3.2. Furnace test

The furnace test was carried out to check the formation of the char layer at temperature of 800 °C and to determine the intumescent factor I of the coatings. Some properties of the char layer after the furnace test were shown in Table 2.

Table 2. Physical properties of char layer after furnace test.

Sample	Weight retention (%)	Adhere to substrate	Intumescent factor I
M-0	23.27	Yes	10.9
M-0.5GR	25.27	Yes	8.3
M-1GR	30.62	Yes	7.1
M-1.5GR	32.54	Yes	6.7
M-2GR	33.38	Yes	6.4

Images of the char layer cross-section after the furnace test are presented in Figure 6. It can be seen that the swelling of the coating tends to decrease with increasing graphene content.

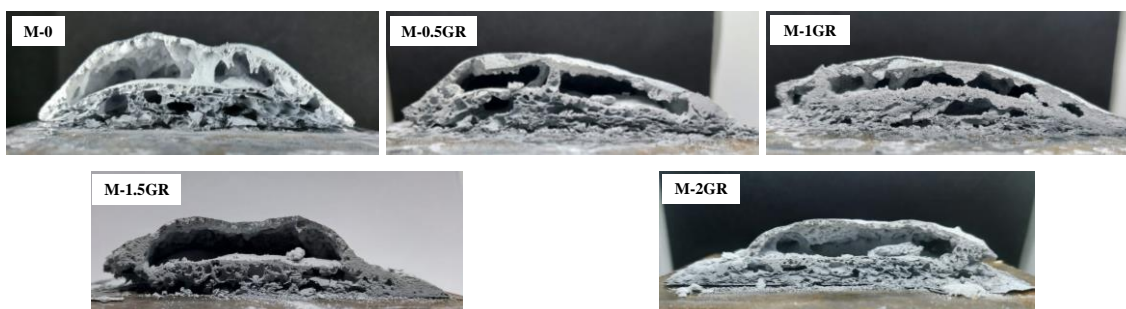


Figure 6. Images of the char layer cross-section after the furnace test.

As shown in Table 2, the weight retention of samples grows with increasing graphene content while intumescent factor I tended to reduce. The literature showed that the char layer significantly impacted fire resistance performance. However, the performance of fire resistance depends on the nature, structure, and content of inorganic additives. Graphene has a two-dimensional layered structure and high thermal stability, which increases the viscosity of the melting coating.

Moreover, graphene having a large specific surface area, could adsorb and/or inhibit the release and diffusion of gases in the combustion process, thus reducing coating expansion in combustion [19, 20]. Figure 6 indicates agreement with this hypothesis. As shown in Figure 6, the char structure of coatings filled with a large amount of graphene was more dense, low expansion, and porous. However, further analysis needs to be conducted to investigate char layer thickness reduction, but fire resistance performance grows with increasing graphene content.

3.3. Morphology of char layer

The fire resistance performance of the coating depends on the structure of the char layer. If the intumescent char layer has a dense structure, it will act as an insulating layer between the substrate material and the flame, increasing fire resistance [21]. The SEM images of char layers after the furnace test are shown in Figure 7.

In Figure 7, the M-0 sample has many cracks and holes observed. These cracks and holes provided convenience for heat and flame to reach the surface of the steel substrate, leading to poor fire resistance. The M-0.5GR sample showed fewer cracks compared to the M-0 sample, resulting in improved fire resistance. Observation of SEM images of char layer samples M-1GR, M-1.5R and M-2GR indicated that the structure of char layers were dense, with few cracks leading to more effective insulation in the fire resistance test.

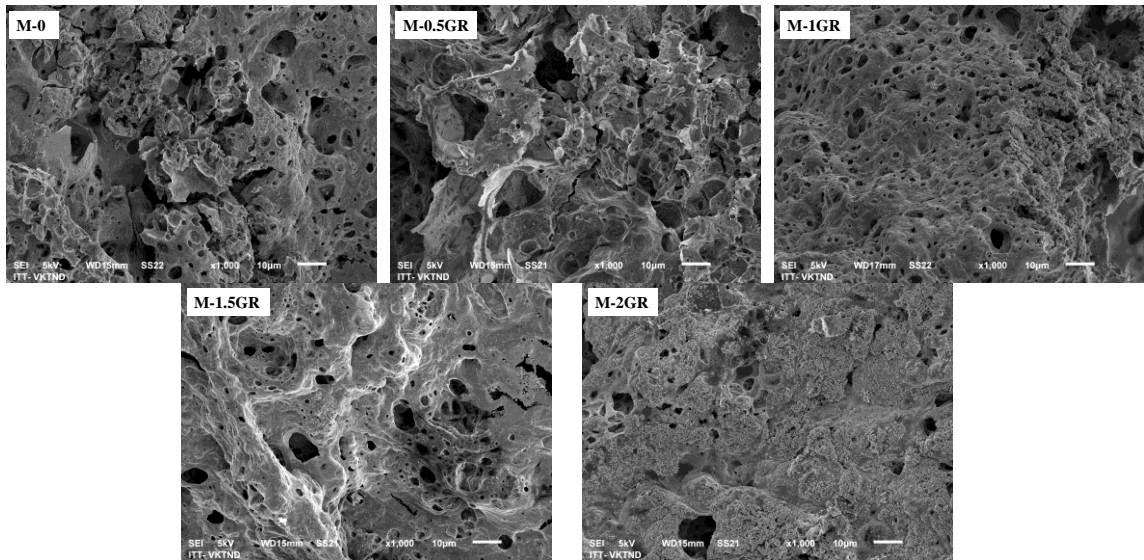


Figure 7. SEM micrograph of the char layer cross-section.

From analyzing the results of SEM images of the char layers, the monolayer structure of graphene has helped to seal, reduce holes and cracks, form a multi-layer protective layer and insulate heat to the protected substrate [10].

3.4. TGA-DSC analysis

The thermogravimetric analysis studied the thermal stability and thermal degradation of the coatings. The TGA curve of the intumescent flame retardant coating samples is presented in Figure 8.

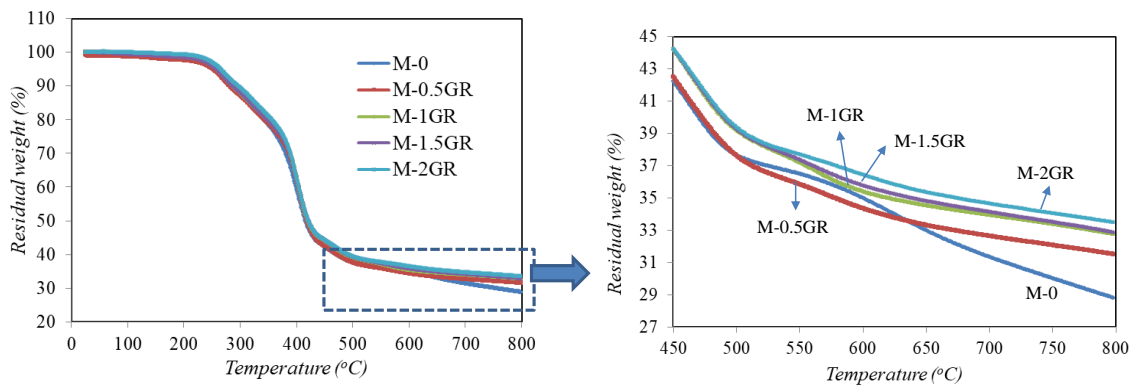


Figure 8. TGA curve of the coatings.

Figure 8 shows that the coatings had similar TGA curves. The thermal degradation of coatings occurred through three stages. In the first stage, from an ambient temperature to 200 °C, water and small molecules of the binder evaporated, causing each coating to lose 2 % weight. Next, in the temperature range from 200 °C to 500 °C, the weight of coating samples decreased rapidly, and the weight loss of samples was fairly stable in the temperature range between 500 and 800 °C. At 800 °C, the residue weights of M-0, M-0.5GR, M-1GR, M-1.5GR and M-2GR

coatings were 28.32 %, 31.25 %, 32.77 %, 32.86 % and 33.50 %, respectively. The residual weight was increased proportionally to the amount of graphene used. It demonstrates that graphene material enhances thermal stability and improves the fire resistance of coatings.

The coating samples M-0 and M-1GR were subjected to differential scanning calorimetry to investigate the decomposition process. The DSC curve of samples were shown in Figure 9.

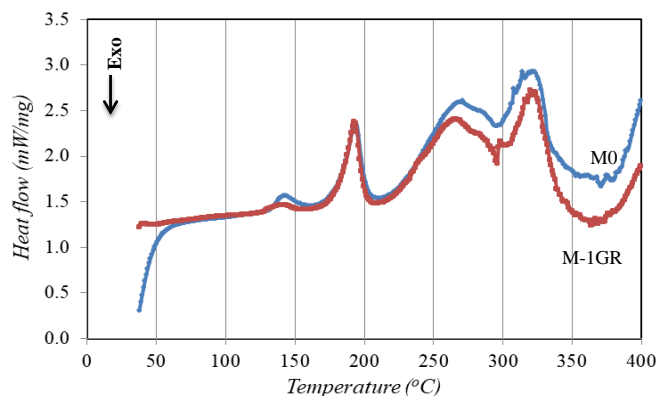


Figure 9. DSC curve of coating samples M-0 and M-1GR.

It can be seen from Figure 9, there is a small endothermic peak at about 140 °C due to the initial melting of acrylic resin. In the temperature range of 170-210 °C, there is an endothermic peak at about 192 °C, which is considered due to the melting of APP and the transformation of the crystal structure of PER.

In the temperature range of 240 - 290 °C, there is a rather large endothermic peak at about 266 °C. This result is thought to be due to the initiation of decomposition of APP when the temperature is raised above 250 °C, releasing phosphoric acid and amines. PER decomposes at this temperature range and reacts with phosphoric acid to form char.

In the temperature range above 300 °C, MEL has just begun to decompose, creating non-flammable gases such as CO₂, N₂. These gases are trapped in the viscous liquid and form bubbles, leading to a blistering coating and thus forming a char layer that protects multiple compartments, acting as an insulating barrier between the flame and the substrate [22, 23].

3.5. Static immersion test

The effects of graphene content on the water resistance of coatings were shown in Figure 10. Figure 10 showed that the weight of coatings increased after 24 hours of immersion and gradually decreased in the following days. In the static immersion test, two processes occur simultaneously: permeation and migration. One of the above two processes will prevail depending on the test time. In the process of permeation, water and corrosive ions infiltrate the coating through the pores of the coating. The permeation process is the cause of the increase in the weight of the coating. At the same time, some hydrophilic flame-retardants (APP, PER and MEL) migrated from the coating to the water, which led to the weight loss of the coating [10].

On the first day of the test, the permeation dominated the migration, resulting in increased weight. In the following days, the migration prevails over the permeation, so the weight began to decrease. When the coatings were immersed for 10 days, permeation and migration reached equilibrium, resulting in little weight change. The weight reduction of the M-0, M-0.5GR, M-

1GR, M-1.5GR and M-2GR after 14 days of testing were 26.67 %, 21.69 %, 17.12 %, 16.1 % and 14.73 %, respectively. These results indicated that graphene increased the water resistance of the coating. The reason might be that graphene material can form parallel arranged structure with a "labyrinth" effect in the coating structure, thus increasing the diffusion path length of OH⁻, H⁺, H₂O and O₂ through the coating. Consequently, water resistance was significantly increased. The schematic of the "labyrinth" effect is presented in Figure 11 [24, 25].

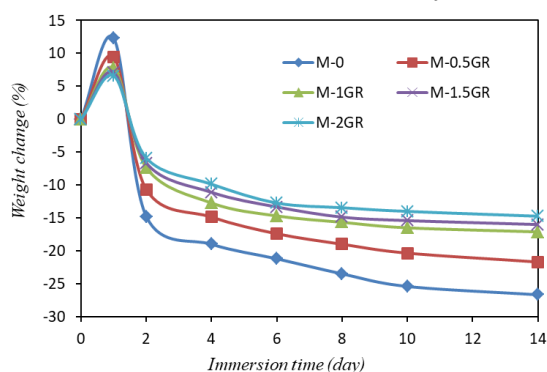


Figure 10. The weight change of the coatings over time of static immersion test.

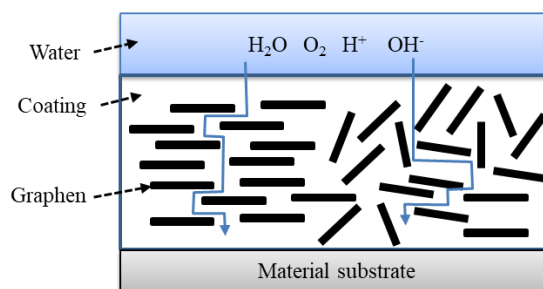


Figure 11. The schematic of the "labyrinth" effect.

3.6. Mechanical properties of coatings

The effect of graphene content on the adhesion and pendulum hardness of the coating was evaluated. The results are presented in Table 3.

Table 3. Relative hardness and adhesion of the investigated coatings.

Properties	M-0	M-0.5GR	M-1GR	M-1.5GR	M-2GR
Adhesion (MPa)	2.23	2.35	2.40	2.44	2.50
Pendulum hardness	0.36	0.39	0.41	0.41	0.42

The results indicated that graphene increased the adhesion and pendulum hardness of the coatings. When compared to the coating without graphene (M-0), the adhesion rose from 5.4 % (M-0.5GR) to 12.1 % (M-2GR). The pendulum hardness of the coating increased from 8.3 % (M-0.5GR) to 16.7 % (M-2GR) compared with the coating without graphene (M-0). This achieved result can be attributed to the Van der Waals force between the graphene layers, which enhances adhesion. At the same time, the layered structure of the graphene layers helps to disperse the impact of the impact force, leading to an increase in the hardness of the coating [22]. However, not every increase in graphene content will increase the mechanical properties.

4. CONCLUSIONS

This study found that graphene is a suitable and effective flame retardant additive for air-absorbent coatings based on emulsion acrylic resins. The graphene presence helps the coating increase fire resistance, thermal stability, water resistance, and mechanical properties.

Based on the results and the relatively expensive cost of graphene, the optimum graphene weight was 1 wt%. Coating with 1 wt% graphene reduced the back surface temperature of the sample by 38 °C, improved water resistance by 9.6 %, adhesion by 7.6 % and pendulum hardness by 13.9 %. The TGA results indicated that adding 1 % graphene increased thermal

stability and the residual weight of the coating from 28.32 % (M-0) to 32.77 % (M-1GR).

Acknowledgements. This work received support from the Annual Financial Fund of the Vietnam Academy of Science and Technology.

CRedit authorship contribution statement. Mac Van Phuc: Formal analysis, Writing & editing. Dao Phi Hung: Formal analysis, Investigation, Review and editing. Nguyen Anh Hiep: Formal analysis, Investigation. Nguyen Thien Vuong: Review and editing. Trinh Van Thanh: Formal analysis.

Declaration of competing interest. The authors have no competing interests.

REFERENCES

1. Mróz K., Hager I., Korniejenko K. - Material solutions for passive fire protection of buildings and structures and their performances testing, *Procedia Engineering* **151** (2016) 284-291. <https://doi.org/10.1016/j.proeng.2016.07.388>.
2. Weil E. D. - Fire-Protective and Flame-Retardant Coatings - A State-of-the-Art Review, *Journal of Fire Sciences* **29** (3) (2011) 259-296. <https://doi.org/10.1177/0734904110395469>.
3. Yasir M., Ahmad F., Yusoff P. S. M. M., Ullah S., and Jimenez M. - Latest trends for structural steel protection by using intumescent fire protective coatings: a review, *Surface Engineering* **36** (4) (2019) 334-363. <https://doi.org/10.1080/02670844.2019.1636536>.
4. Wang G., Yang J. - Influences of binder on fire protection and anticorrosion properties of intumescent fire resistive coating for steel structure, *Surface and Coatings Technology* **204** (8) (2010) 1186-1192. <https://doi.org/10.1016/j.surfcoat.2009.10.040>.
5. Jimenez M., Duquesne S., Bourbigot S. - Intumescent fire protective coating: Toward a better understanding of their mechanism of action, *Thermochimica Acta* **449** (1–2) (2006) 16-26. <https://doi.org/10.1016/j.tca.2006.07.008>.
6. Lucherini A., Maluk C. - Intumescent coatings used for the fire-safe design of steel structures: A review, *Journal of Constructional Steel Research* **162** (2019) 105712. <https://doi.org/10.1016/j.jcsr.2019.105712>.
7. Xue Y., Zhang S., Yang W. - Influence of expanded vermiculite on fire protection of intumescent fireproof coatings for steel structures, *Journal of Coatings Technology and Research* **12** (2) (2014) 357-364. <https://doi.org/10.1007/s11998-014-9626-3>.
8. Martins M. S. S., Scharrel B., Magalhães F. D., & Pereira C. M. C. - The effect of traditional flame retardants, nanoclays and carbon nanotubes in the fire performance of epoxy resin composites, *Fire and Materials* **41** (2) (2016) 111-130. <https://doi.org/10.1002/fam.2370>.
9. Nasir K. M., Sulong N. H. R., Johan M. R., and Afifi A. M. - Synergistic effect of industrial- and bio-fillers waterborne intumescent hybrid coatings on flame retardancy, physical and mechanical properties, *Progress in Organic Coatings* **149** (2020) 105905. <https://doi.org/10.1016/j.porgcoat.2020.105905>.
10. Zhan W., Chen L., Cui F., Gu Z., and Jiang J. - Effects of carbon materials on fire protection and smoke suppression of waterborne intumescent coating, *Progress in Organic Coatings* **140** (2020) 105491. <https://doi.org/10.1016/j.porgcoat.2019.105491>.
11. Hu R., Chu L., Zhang J., Li X., & Huang W. - Carbon materials for enhancing charge transport in the advancements of perovskite solar cells. *Journal of Power Sources*, **361** (2017) 259-275. <https://doi.org/10.1016/j.jpowsour.2017.06.051>.
12. Wei H., Zhu Z., Sun H., Mu P., Liang W., and Li A. - Graphene and poly(ionic liquid)

- modified polyurethane sponges with enhanced flame- retardant properties, *Journal of Applied Polymer Science* **134** (44) (2017) 45477. <https://doi.org/10.1002/app.45477>.
13. Stankovich S., Dikin D., Dommett G., Kevin M. Kohlhaas, Eric J. Zimney, Eric A. Stach, Richard D. Piner, Son Binh T. Nguyen, and Rodney S. Ruoff - Graphene-based composite materials, *Nature* **442** (2006) 282-286. <https://doi.org/10.1038/nature04969>.
 14. Phiri J., Gane P., Maloney T. C. - General overview of graphene: Production, properties and application in polymer composites, *Materials Science and Engineering: B* **215** (2017) 9-28. <https://doi.org/10.1016/j.mseb.2016.10.004>.
 15. Yuan B., Sun Y., Chen X., Shi Y., Dai H., He S. - Poorly-/well-dispersed graphene: Abnormal influence on flammability and fire behavior of intumescent flame retardant, *Composites Part A: Applied Science and Manufacturing* **109** (2018) 345-354. <https://doi.org/10.1016/j.compositesa.2018.03.022>.
 16. Zhan W., Chen L., Gu Z., Jiang J. - Influence of graphene on fire protection of intumescent fire retardant coating for steel structure, *Energy Reports* **6** (2020) 693-697. <https://doi.org/10.1016/j.egyr.2019.11.139>.
 17. Hung D. P., Quan V. A., Thanh T. V., Hiep N. A., Vuong N. T., Phuc M. V. - Mechanical, thermal properties and morphology of composite coating based on acrylic emulsion polymer and graphene oxide, *Vietnam Journal of Science and Technology* **58** (2) (2020) 228-236. <https://doi.org/10.15625/2525-2518/58/2/13932>.
 18. Aziz H., Ahmad F. - Effects from nano-titanium oxide on the thermal resistance of an intumescent fire retardant coating for structural applications. *Progress in Organic Coatings* **101** (2016) 431-439. <https://doi.org/10.1016/j.porgcoat.2016.09.017>.
 19. Giang L. T., Hanh D. T., Ha T. T. - Flame retardants appear and exist in indoor gaseous environments, *Natural Science and Technology Publisher, Ha Noi, 2020* (in Vietnamese).
 20. Fan F. Q., Xia Z. B., Li Q. Y., Li Z. - Effects of inorganic fillers on the shear viscosity and fire retardant performance of waterborne intumescent coatings, *Progress in Organic Coatings* **76** (5) (2013) 844-851. <https://doi.org/10.1016/j.porgcoat.2013.02.002>.
 21. Wang Z., Han E., Ke W. - Effect of nanoparticles on the improvement in fire-resistant and anti-ageing properties of flame-retardant coating, *Surface and Coatings Technology* **200** (20–21) (2006) 5706-5716. <https://doi.org/10.1016/j.surfcoat.2005.08.102>.
 22. Zhan W., Ni L., Gu Z., Cui F., Jiang J., Chen L. - The influences of graphene and carbon nanotubes on properties of waterborne intumescent fire resistive coating, *Powder Technology* **385** (2021) 572-579. <https://doi.org/10.1016/j.powtec.2021.03.018>.
 23. Zhan W., Gu Z., Jiang J., Chen L. - Influences of surface area of graphene on fire protection of waterborne intumescent fire resistive coating, *Process Safety and Environmental Protection* **139** (2020) 106-113. <https://doi.org/10.1016/j.psep.2020.04.004>.
 24. Mohammadi S., Roohi H. - Influence of functionalized multi-layer graphene on adhesion improvement and corrosion resistance performance of zinc-rich epoxy primer, *Corrosion Engineering, Science and Technology* **53** (6) (2018) 422-430. <https://doi.org/10.1080/1478422x.2018.1495679>.
 25. Anees S. M., Dasari A. - A review on the environmental durability of intumescent coatings for steels, *Journal of Materials Science* **53** (1) (2017) 124-145. <https://doi.org/10.1007/s10853-017-1500-0>.